VALIDATION AND IMPROVEMENTS OF A MESOSCALE FINITE ELEMENT CONSTITUTIVE MODEL FOR FIBRE KINKING GROWTH

S. Costa[1,2], M. Fagerström[2] , R. Gutkin[3], R. Olsson[1]

[1]Swerea SICOMP, Mölndal, Sweden
[2] Chalmers Univ. of Technology, Depart. of Industrial and Materials Science, Gothenburg, Sweden
[3]Volvo car corporation

Keywords: Fibre kinking, Crash, Continuous damage modelling, FEM

Abstract
The present work is focused on the computational challenges and further verification and validation of an advanced fibre kinking model. This model was previously developed by the authors and implemented in a Finite Element (FE) code with a mesh objective formulation. The previous validation in terms of comparison with an analytical and a micromechanical model is herein extended to also encompass FE simulations of longitudinal compression in multiaxial stress states. In addition, numerical improvements have been added to the model targeting its computational efficiency and stability in order to handle multiaxial stress states and large structures.

1. Introduction

Accurate constitutive models are fundamental for efficient designs. The crash of composite materials has a lot to benefit from efficient models due to the design freedom that can be explored such as fibre architecture, type of composites, and geometry of the part. To develop such a model we need a deep knowledge of the mechanisms involved. The kink-band formation is the mechanism that can absorb most energy. It has been extensively investigated experimentally for uniaxial loading [1] as well as for kinking under biaxial loading [2]. Several models have been proposed, from analytical to micromechanical [3] and mesoscale/ply level models.

The mesoscale constitutive model being further validated here [4,5] is a physically based model at the ply level that includes fibre rotation and the nonlinear shear behaviour due to growth of microcracks with friction. The stress-strain relation predicted by the current model was already validated by comparison against two experimental test cases as well as against analytical and numerical models where it successfully predicted the compression strength at the right strain and the subsequent crush stress [4]. The FE implementation also yields a mesh objective response [5]. However the past verifications only involved nearly uniaxial loading. In the current work we extend the validation to biaxial stress states.

Validation of models for fibre kinking growth is a challenging task due to the instability of kink band development. Even for uniaxial crushing of simple specimens the fibre kinking phenomena are not completely isolated from other mechanisms such as splaying [6]. A meaningful validation requires that distinctive multiaxial load cases are successfully simulated. In this paper we study a single element under multiaxial stress states and a dog bone specimen where shear influences the kinking response, thus validating the additional improvements on speed and robustness added to handle large structures.

2. Model overview

In order to have an overall understanding of computational challenges associated with the model we present a succinct summary of the equations. Further details about the development of the current 3D model are explained in detail in [4,5,7]. To determine both the longitudinal response and the shear angle in a physically based way it is necessary to solve simultaneously:

I. The strain compatibility between the global and misaligned frame;

II. The stress equilibrium;

III. The nonlinear shear response of the matrix supporting the fibres.

Assuming that the fibres have an initial misalignment and rotate further under stresses and strains, the equilibrium between the misaligned frame *m* and the global frame can be established. Thus, the strain compatibility (I) conditions have to be satisfied to ensure continuity when the body is deformed. The strain compatibility equation for the longitudinal component can be expressed as a function of the shear angle and the strains in the kink-band coordinate system or here called misalignment frame as follows:

$$\begin{aligned} &\varepsilon_{11} = \left[\varepsilon_{11}^m + \varepsilon_{22}^m + \left(\varepsilon_{11}^m - \varepsilon_{22}^m\right)\cos(2\theta) - \gamma_{12}^m \sin(2\theta)\right]/2 \\ &\text{where} \quad \theta = \gamma_{12}^m + \theta_i \end{aligned} \tag{1}$$

and θ_i is the initial misalignment. Furthermore, the strains expressed in the misalignment frame, ε_{11}^m and ε_{22}^m, can be related with the stresses using transverse isotropy as

$$\varepsilon_{11}^m = \frac{\sigma_{11}^m}{E_{11}} - \frac{\nu_{21}\sigma_{22}^m}{E_{22}} - \frac{\nu_{31}\sigma_{33}^m}{E_{33}} \qquad \varepsilon_{22}^m = \frac{\sigma_{22}^m}{E_{22}} - \frac{\nu_{12}\sigma_{11}^m}{E_{11}} - \frac{\nu_{32}\sigma_{33}^m}{E_{33}} \tag{2}$$

The two unknowns from transverse isotropy are the stresses, σ_{11}^m and σ_{22}^m obtained from the stress equilibrium (II) between the global and the local frame:

$$\begin{aligned} \sigma_{11}^m &= \frac{\sigma_{11}+\sigma_{22}}{2} + \frac{\sigma_{11}-\sigma_{22}}{2}\cos(2\theta) + \tau_{12}\sin(2\theta) \\ \sigma_{22}^m &= \frac{\sigma_{11}+\sigma_{22}}{2} - \frac{\sigma_{11}-\sigma_{22}}{2}\cos(2\theta) - \tau_{12}\sin(2\theta) \end{aligned} \tag{3}$$

where the stresses without subscript are in the global coordinate frame. The third equation of the stress equilibrium (the shear stress in the kink band, τ_{12}^m) can be re-arranged to obtain the longitudinal response or the fibre kinking stress as

$$\sigma_{11} = \sigma_{22} + 2\frac{\tau_{12}\cos(2\theta) - \tau_{12}^m}{\sin(2\theta)} \tag{4}$$

The transverse and the shear stress, σ_{22} and τ_{12} respectively, need to be calculated from the nonlinear response of the matrix (III), detailed in [8]. The nonlinear shear response is obtained by combining damage and friction [8] as follows

$$\tau_{12}^m = G_{12}\gamma_{12}^m(1-d) + d\,\tau^{friction} \quad \text{where} \quad \tau^{friction} = \begin{cases} G_{12}\left(\gamma_{12}^m - \gamma_{12old}^m\right) & \text{if no sliding} \\ \mu_L\left\langle \sigma_{22}^m - p_{0L}\right\rangle_- & \text{if sliding} \end{cases} \tag{5}$$

where $\tau^{friction}$ represents the in-plane frictional stress. The dissipative mechanisms are represented by damage, *d* and the previous shear strain, γ_{12old}^m. The equations (1)-(5) are solved for γ_{12}^m using

numerical methods. Once the shear angle is obtained with a tight tolerance the fibre kinking stress σ_{11} of interest is also obtained.

The model accounts for the initial fibre misalignment and the influence of the transverse stresses, as shown in Figure 1(a). The model is able to predict the whole kinking response, accounting for higher stiffness and peak stress for lower initial misalignments. The failure is predicted by shear instability being more abrupt (unstable) for lower initial misalignments, Figure 1(b).

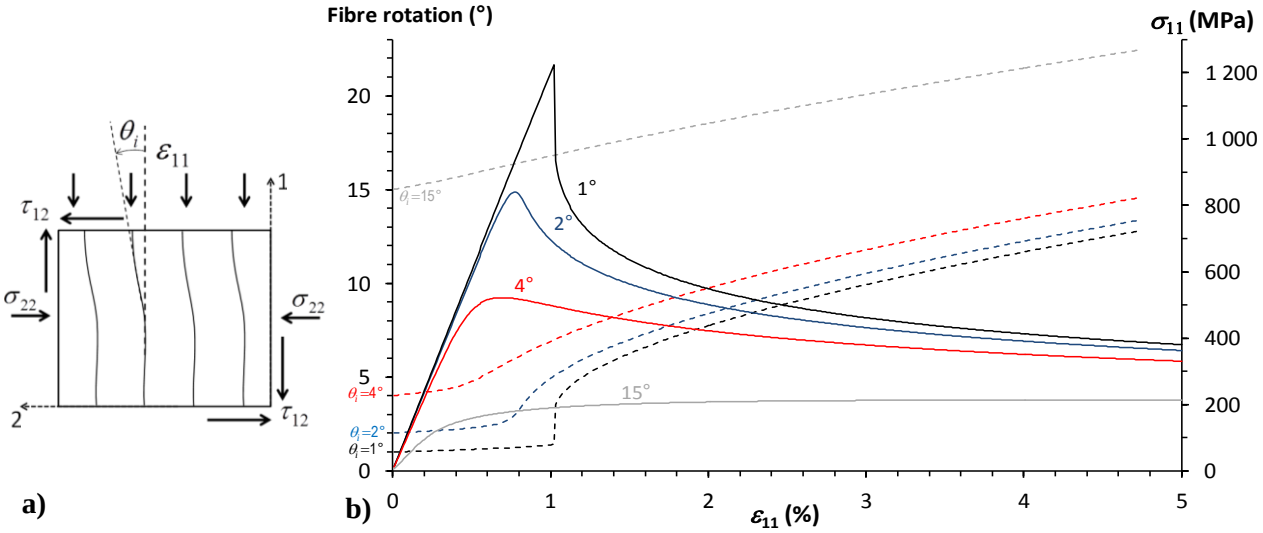

Figure 1.a) Illustration of the stress state influencing the in-plane kink band growth; b) Analytical prediction of stresses and fibre rotation for 1°, 2°, 4° and 15° of initial misalignment [5].

The material properties used here are similar to the ones reported in Costa et al. [5]. Using common notation for composites we assume the following elastic properties (units in GPa): $E_{11}=136, E_{22}=9.15, E_{33}=7.7, G_{12}=4.4, G_{23}=3.02, G_{13}=3.7$ and the Poisson's ratio as: $\nu_{12}=\nu_{13}=0.28, \nu_{23}=0.43$. The onset of nonlinearity in the shear response is estimated visually from the in-plane shear response as $\tau_{0L}=23\text{MPa}$. The parameters used to obtain the nonlinear shear response are $p = -0.6$ calibrated with the shear stress-strain curve, the coefficient of friction $\mu_L=0.4$ and the internal pressure is $p_{0L}=60\text{MPa}$.

3. Computational aspects

Failure dominated by fibre kinking is very unstable by nature. The current model accounts well for a very sudden failure once the peak stress is reached. These physically based characteristics come with high difficulties in stabilizing the model. In order to obtain an acceptably stable simulation without affecting the results we investigated different formulation of the hourglass control, using FORTRAN with double precision, different strain formulation of our model and varying the tolerance of the bisection method. Even though the results were influenced none of the approaches significantly improved the results. More stability could be achieved for a tolerance of approximately $2\text{x}10^{-7}$, the default hourglass formulation, and double precision. Double precision is important due to truncation errors that are an issue for explicit simulations with many increments. Having a root-finding method inside an explicit simulation requires extra care with the numerical approximations due to the very different numbers involved (such as stresses and strains) making them much more vulnerable to rounding errors. Thus all the code was implemented using double precision. The most suitable strain formulation is still under investigation. The speed was also investigated showing that higher improvements could be achieved by shortening the search interval of the bisection method when

compared to typically faster convergence methods such as Newton-Raphson. All the values that do not depend on gamma are also removed from the bisection. We also take advantage of the repetitive terms to calculate them only once inside the bisection method, such as the cosines and sines.

3.1 Interval of the bisection

The bisection method is very computationally cumbersome and therefore one can achieve big gains by reducing the number of iterations. Thus, the interval for the bisection method, *a* and *b* are shortened based on the shear angle from previous increment γ_{12old}^{m} as follows

$$\begin{aligned} a &= \max\left(0, \gamma_{12old}^{m} - 0.05\right) \\ b &= \gamma_{12old}^{m} + 0.05 \end{aligned} \tag{6}$$

where 0.05 subtracted from *a* and added to *b* was found to be appropriate and reduce the number of interactions substantially. Reducing the interval of bisection increases the speed of the simulation by 15-20% for the dog bone specimen for example. Further studies on an automatic interval that can be even smaller will be investigated in the future.

3.2 Handling exceptions

To deal with multiaxial stress states and to be able to simulate large structures it was necessary to handle exceptions. There are combinations of stress states and strain states that do not have a physical solution using the current fibre kinking model. Using the proposed fibre kinking model only for negative longitudinal strains does not always guarantee a solution. For example for situations with tiny compressive strains under transverse compressive stresses is not possible to obtain gamma in an interval between 0 and 1. In a large structure is more likely to find situations without solution. Therefore a criterion for handling exceptions is proposed as follows:

$$if \quad \begin{Bmatrix} \gamma_{12}^{m} \le |a| + tol \\ \gamma_{12}^{m} \ge |b| - tol \end{Bmatrix} \quad \text{then } \gamma_{12}^{m} = \gamma_{12old}^{m} \tag{7}$$

Using the previous value of gamma avoids the simulation to crash when the gamma does not exist in the given interval.

3.3. Criterion for fibre kinking onset

Further speed gains can be achieved by using the fibre kinking theory only when a certain criterion is met. A suitable criterion for onset of shear nonlinearity is necessary. The nonlinear shear response is given using the transformation equations as

$$\tau_{12}^{m} = -\frac{\sigma_{11} - \sigma_{22}}{2}\sin(2\theta) + \tau_{12}\cos(2\theta) \tag{8}$$

Before nonlinearity starts the rotations θ are small and the previous equation can be simplified without significant errors by assuming small angle approximations:

$$G_{12}\gamma_{12}^{m} \approx \left(\sigma_{22} - \sigma_{11}\right)\left(\theta_i + \gamma_{12}^{m}\right) + \tau_{12} \tag{9}$$

For linear shear behaviour the shear strain in the misalignment frame can be solved as

$$\gamma_{12}^{m} = \frac{\theta_i(\sigma_{22} - \sigma_{11}) + \tau_{12}}{G_{12} + \sigma_{11} - \sigma_{22}} \tag{10}$$

The starting of nonlinearity is defined as τ_{0L}. When the shear strain is larger than the shear strain at the start of nonlinearity the Fibre kinking criterion is activated

$$if \ \left|\gamma_{12}^{m}\right| > \frac{\tau_{0L}}{G_{12}} \ then \ \text{call fibre-kinking} \tag{11}$$

Using this criterion will result in fibre kinking being activated only in the necessary locations which evidently can speed up the simulation considerably. However, the consequences of using the fibre kinking model only locally were not investigated here and will be addressed in future work.

4. Validation for multiaxial stress states

4.1. Single element

In order to validate the multiaxial nature of fibre kinking as demonstrated by [9] we verified the model response using a single element subjected to shear and transverse loading as well as transversely constrained, Figure 2.

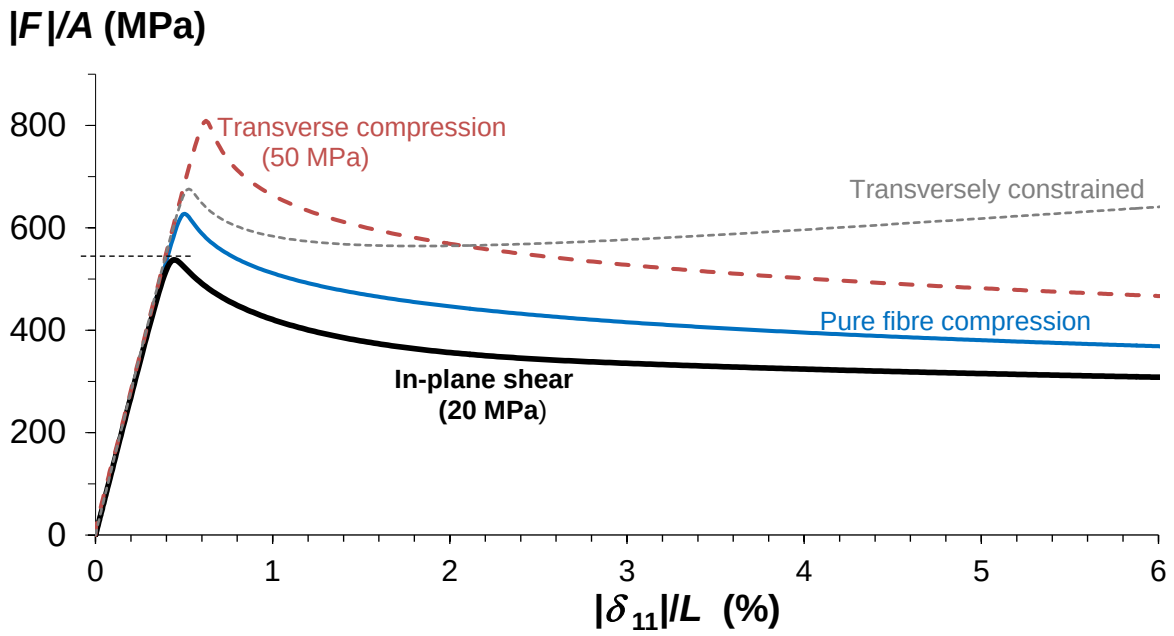

Figure 2. Element test of the model behaviour under different load scenarios and BCs

The results show that even small values of positive shear are able to lower the whole kinking response while transverse compression results in higher kinking stresses. Constraining the model on the sides increases slightly the peak stress and causes an increasing stiffness during the subsequent damage growth. Thus, the model response is as expected for a single element.

4.2. Dog bone specimen

A specimen that fails less catastrophically in kinking is the dog bone specimen due to the raise of in-plane shear on the sides that trigger the kinking response. Therefore this specimen is used for validation of the robustness. The specimen was modelled in Abaqus with C3D8R elements. A simple support BC is applied and a displacement is introduced on the top. The results for the shear stress and the damage growth are shown if Figure 3.

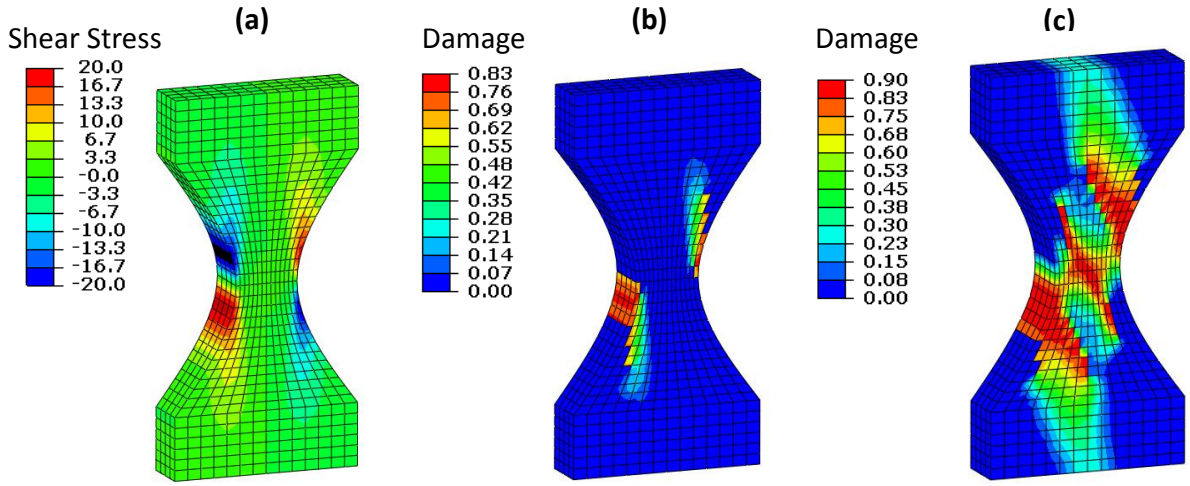

Figure 3. Influence of the shear stresses in kinking formation and growth

The model predicts kinking initiation in the areas of positive shear only. At a later stage a larger kink-band crosses the whole specimen. The stress-strain response can be observed in Figure 4, where the three stages shown in figure 3 are represented by red squares.

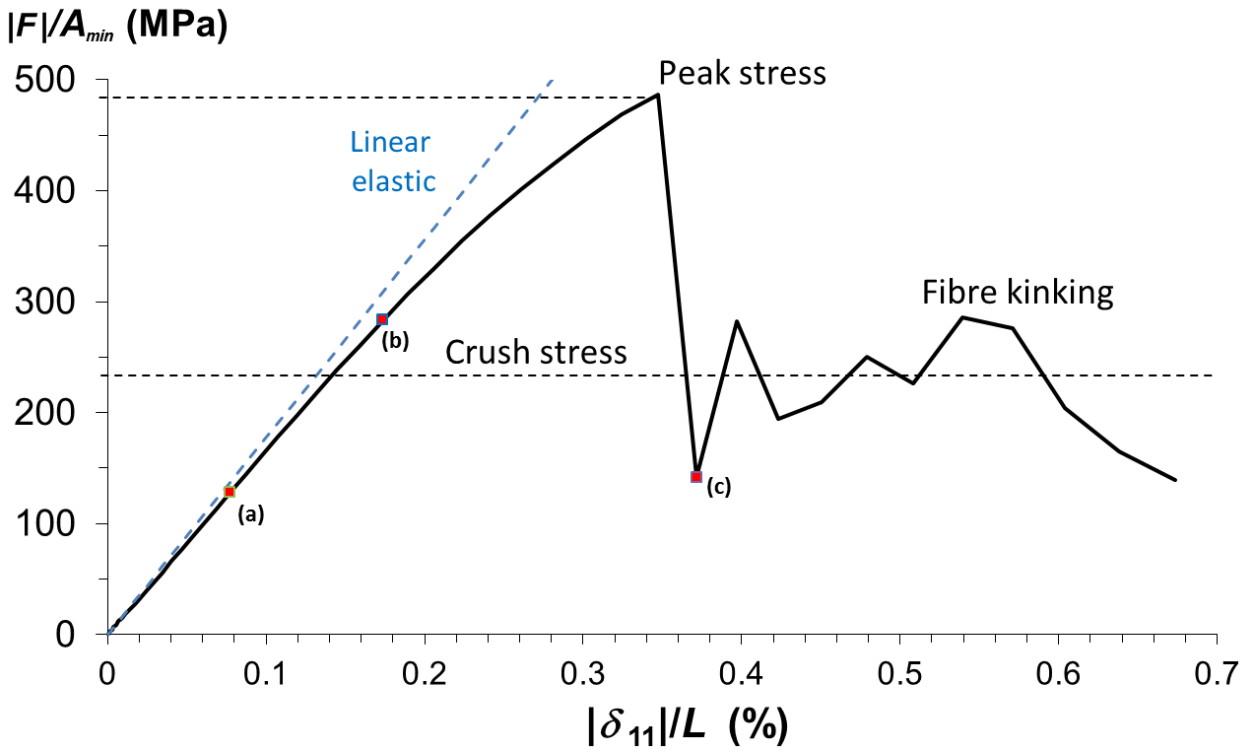

Figure 4. Compressive response of the dog bone specimen, apparent stress vs. apparent strain

One can observe that the peak strength does not correspond to the onset of yielding as reported in the literature [3,10]. The peak stress also occurs at lower strength than the predicted by the model for a pure compression case. The lower strength for the dog bone is attributed to the influence of the shear stresses. Once fibre kinking occurs, i.e. during kink-band development, the response is similar to the crush stress reported in [6], followed by a decrease of stresses.

It is worth to point out that the kinking model predicts a decrease in stiffness even before the peak stress is reached. This is related with damage growth of the matrix supporting the rotated fibres. A decrease of stiffness before the peak stress is also observed experimentally.

5. Future work and conclusions

Assuming that the initial misalignment angle is always positive does not reflect the waviness nature of fibre composites. For this reason a positive shear can either decrease the kinking stress or increase it. Future model developments also need to consider both negative and positive shear strains.

A model for the kink-band formation and growth was presented. It was demonstrated that the model implemented in Abaqus captures well the influence of transverse and shear stresses as well as the influence of constrained BCs. These model capabilities are shown in more complex specimens such as the dog bone specimen.

Acknowledgments

This work was supported by the Swedish Energy Agency [project number 34181-2]; and FFI/VINNOVA [dnr 2016-04239]. The discussions with Thomas Bru and Daniel Berglund at Swerea SICOMP AB as well as with Victor de la Mora at TU Delft are gratefully acknowledged.

References

[1] Wilhelmsson D. On matrix-driven failure in unidirectional NCF composites. Tekn. Lic Thesis. Chalmers Univ of Techn, Gothenburg, 2016.
[2] Edgren F, Asp LE, Joffe R. Failure of NCF composites subjected to combined compression and shear loading. Compos Sci Technol 2006;66:2865–77.
[3] Pimenta S, Gutkin R, Pinho ST, Robinson P. A micromechanical model for kink-band formation: Part I — Experimental study and numerical modelling. Compos Sci Technol 2009;69:948–55.
[4] Gutkin R, Costa S, Olsson R. A physically based model for kink-band growth and longitudinal crushing of composites under 3D stress states accounting for friction. Compos Sci Technol 2016;135:39–45.
[5] Costa S, Gutkin R, Olsson R. Mesh objective implementation of a fibre kinking model for damage growth with friction. Compos Struct 2017;168:384–91.
[6] Bru T, Waldenström P, Gutkin R, Olsson R, Vyas GM. Development of a test method for evaluating the crushing behaviour of unidirectional laminates. J Compos Mater 2017;51:4041–51.
[7] Costa S, Gutkin R, Olsson R. Finite element implementation of a model for longitudinal compressive damage growth with friction. ECCM 2016 - Proceeding 17th Eur Conf Compos Mater, 2016.

[8] Gutkin R, Pinho ST. Combining damage and friction to model compressive damage growth in fibre-reinforced composites. J Compos Mater 2015;49:2483–95.
[9] Basu S, Waas AM, Ambur DR. Compressive failure of fiber composites under multi-axial loading. J Mech Phys Solids 2006;54:611–34.
[10] Davidson P, Waas a. M. Mechanics of kinking in fiber-reinforced composites under compressive loading. Math Mech Solids 2014:1–18.